Field-Field and Photon-Photon Correlations of Light Scattered by Two Remote Two-Level InAs Quantum Dots on the Same Substrate

K. Konthasinghe,[1] M. Peiris,[1] Y. Yu,[2] M. F. Li,[2] J. F. He,[2] L. J. Wang,[2] H. Q. Ni,[2] Z. C. Niu,[2] C. K. Shih,[3] and A. Muller[1,*]

[1]*Department of Physics, University of South Florida, Tampa, Florida 33620, USA*

[2]*Institute of Semiconductors, Chinese Academy of Sciences, Beijing 100083, People's Republic of China*

[3]*Department of Physics, University of Texas at Austin, Austin, Texas 78712, USA*

(Received 16 July 2012; published 28 December 2012)

We report the measurement of field-field and photon-photon correlations of light scattered by two InAs quantum dots separated by ≈ 40 μm. Near 4 K a large fraction of photons can be scattered coherently by each quantum dot leading to one-photon interference at a beam splitter (visibility $\approx 20\%$). Simultaneously, two-photon interference is also observed (visibility $\approx 40\%$) due to the indistinguishability of photons scattered by the two different quantum emitters. We show how spectral diffusion accounts for the reduction in interference visibility through variations in photon flux.

DOI: 10.1103/PhysRevLett.109.267402 PACS numbers: 78.67.Hc, 78.47.−p, 78.55.Cr

Introduction.—Interference is at the heart of all optical phenomena, epitomized by Young's double-slit experiment, a classical wave effect. In quantum optics, it is the probability amplitudes of photon trajectories that interfere, not the photons themselves. As an analogy to Young's experiment, Eichmann *et al.* first observed fringes on a screen positioned at a fixed distance from two trapped ions due to one-photon interference [1]. In contrast to Young's classical experiment, however, interference fringes could be observed only at low laser intensities, at which the photons are scattered coherently in the absence of absorption and reemission [2]. Quantum mechanically, if an ion were to undergo a transition to its excited state during the scattering process, it would become possible to determine which of the two ions emitted the photon. Thus, such a case should not yield any interference fringes.

Despite an absence of one-photon interference, however, two-photon interference may still be observed. Hong *et al.* first showed that single photons with indistinguishable spatial properties, temporal properties, and polarizations impinging simultaneously on a 50/50 beam splitter always exit together due to an interference of probability amplitudes [3]. This type of interference, now verified extensively with atoms [4,5], ions [6], single molecules [7], and solid-state quantum emitters [8–12], is expected to play an important role in the realization of quantum networks, in which remote, often dissimilar, quantum systems must be connected [13]. While one-photon interference may be observed using classical sources, two-photon interference requires quantum light sources, although the latter does not preclude the former.

We show here that near-resonant light scattering from two solid-state two-level systems exhibits both one-photon and two-photon interference. The two-level systems we use are InAs quantum dots (QDs) in the same semiconductor chip separated by ≈ 40 μm. In contrast to prior two-photon interference measurements using photoluminescence [9–12], identical resonance frequencies for the two emitters are not required because, by virtue of the scattering process, the emission spectrum is centered at the laser frequency, not the natural frequency of the two-level system [2]. We show that in fact the scattered light spectra for the two QDs can have large overlap provided the laser frequency is suitably chosen to lie in between the resonance frequencies of the two QD transitions. Under such conditions, the only limiting factor to sizable interference fringe visibility is spectral diffusion, which causes flickering of the scattered light intensity. A simple statistical analysis provides close agreement with our experimental observations of one-photon ($\approx 20\%$) and two-photon ($\approx 40\%$) visibilities.

Experiments.—Our sample, containing InAs QDs at the center of a planar optical microcavity, is described in Ref. [14]. With narrow linewidths [15], InAs QDs have revealed unique features of a quantum-coherent system, such as the Mollow triplet [16–20]. Figure 1 illustrates our experiment for probing interference of light scattered by two spatially separated QD emitters, labeled "QDL" and "QDR" at $T = 3.8$ K. In each QD, the transition from a ground ($|0\rangle$) to an excited ($|1\rangle$) state (natural frequency ω_0) is near resonant with an incident monochromatic laser of frequency ω [Fig. 1(a)]. Here, state $|1\rangle$ is a neutral excitonic state. The light scattered by QDL and QDR is separated, recombined at a beam splitter, and analyzed by two single photon detectors and photon counting instrumentation.

The spectral characteristics of QDL and QDR are shown in Fig. 2. As is seen in an image of the sample surface [Fig. 2(a)], the QDs are separated by about 40 μm and are well isolated from any background scatterers. The excitation spectra of Fig. 2(b), obtained by scanning the laser frequency and recording the total scattered light intensity, further reveal that the resonance frequencies

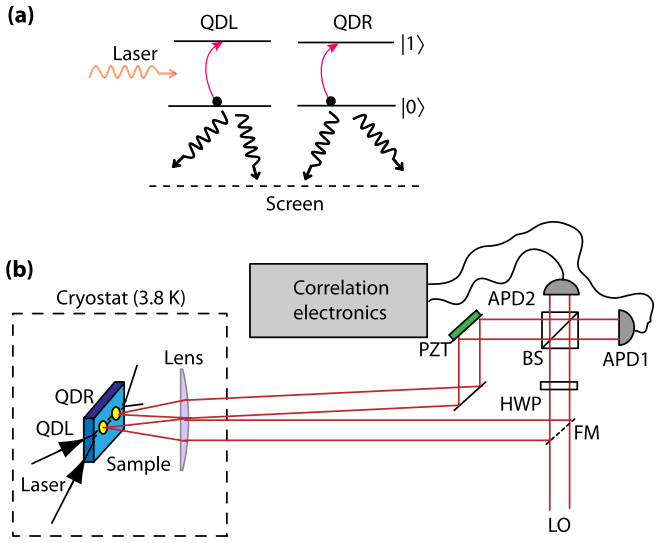

FIG. 1 (color online). (a) Schematic of two-QD scattering experiment. In the classical Young's experiment the scattered light intensity is impinging on a screen recording spatial interference fringes. (b) Experimental setup with the QD sample inside a cryostat with optical access. An *in situ* lens separates the scattered light from "QDL" and "QDR" which is then recombined at a nonpolarizing 50/50 beam splitter (BS). The relative phase of the two waves is controlled with a piezoelectric actuator (PZT). Avalanche photon counting detectors (APD) record events at the beam splitter outputs. A flip mount (FM) allows us to replace one of the QD signals with a reference local oscillator (LO). For polarization control, a half wave plate (HWP) is inserted into one of the arms.

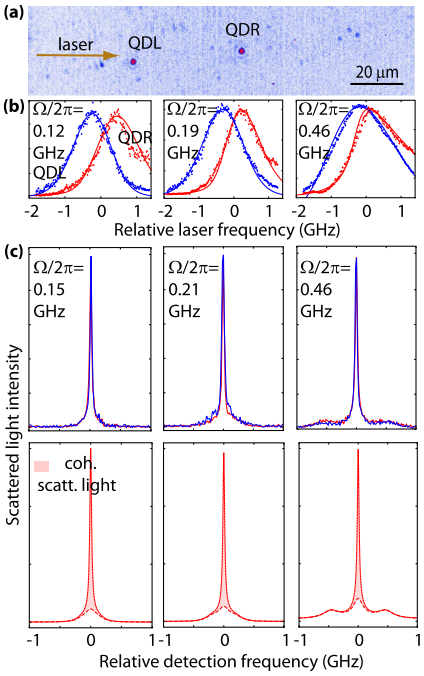

FIG. 2 (color online). (a) Image of sample surface showing the two QDs investigated. (b) Excitation spectra for QDL (red trace) and QDR (blue trace) at several Rabi frequencies. (c) Corresponding experimental (top) and theoretical (bottom) high-resolution spectra of the scattered light at $\Delta\omega/2\pi = 0.3$ GHz. At saturation, i.e., when $\Omega = \kappa/\sqrt{2}$, the laser power before entering the cryostat was 4 μW.

of QDL and QDR differ by about 0.6 GHz. Even under power-broadened conditions, the overlap of the two spectra is modest. Here the Rabi frequency Ω was increased by increasing the laser intensity. However, despite this incomplete overlap, the spectra of the light scattered by QDL and QDR, shown in Fig. 2(c), are almost identical when the laser detuning, $\Delta\omega = \omega - \omega_0$, is suitably chosen; i.e., $\Delta\omega_{\mathrm{QDL}} = -\Delta\omega_{\mathrm{QDR}}$ when $\Omega_{\mathrm{QDL}} = \Omega_{\mathrm{QDR}}$. The spectra of Fig. 2(c) show the familiar evolution from coherent to incoherent scattering [14,21,22].

One-photon interference was investigated by recording field-field correlations via the light intensity at the output of the beam splitter in Fig. 1(b). The relative path length traveled by the light scattered by QDR was varied with a piezoelectric actuator. The resulting fringe contrast, obtained as the difference between the intensities at the beam splitter outputs divided by their sum, is shown in Fig. 3. When interfering the signals from the two QDs [Figs. 3(a)–3(c)], fringe contrasts are as large as 20%, whereas replacing one of the inputs with a local oscillator [Figs. 3(d)–3(f)] increases the fringe contrast to about 50%. Note that in photoluminescence experiments, which lack a well-defined phase relationship between the incident laser and the emitted light, no such interference is ever possible. It is the coherent part of the scattered light, illustrated by the shaded part of the spectra in Fig. 2(c), that gives rise to the fringes.

Two-photon interference was investigated by recording correlations between photons from the two beam splitter output ports. Experimental second-order correlation functions, $g^{(2)}(\tau)$, are shown in Fig. 4, for light from each QD alone [Fig. 4(a)], for light from both QDs with parallel polarizations [Fig. 4(b)], and for light from both QDs with perpendicular polarizations [Fig. 4(c)]. The raw interference visibility is as large as 44%, but is limited here by $g_{\parallel}^{(2)}(0)$, which is increased from zero primarily due to the detectors' finite resolution. The detectors' instrument response function (IRF), shown in the upper left-hand panel of Fig. 4(a), has been convolved with the theoretically expected $g^{(2)}(\tau)$ to obtain the solid lines in Fig. 4(a) [14].

Both one-photon (Fig. 3) and two-photon (Fig. 4) interference visibilities differ significantly from those expected from two ideal radiatively broadened two-level quantum systems. For the former we expect almost unity fringe contrast at sufficiently low laser power, i.e., when most of the light is scattered coherently. For the latter, we expect $g_{\perp}^{(2)}(\tau) \approx 0.5$ and $g_{\parallel}^{(2)}(\tau) \approx 0$. Nonetheless, the data of Figs. 3 and 4 provide for the first time clear evidence of strong coalescence of two single photons resonantly scattered from two remote solid-state emitters.

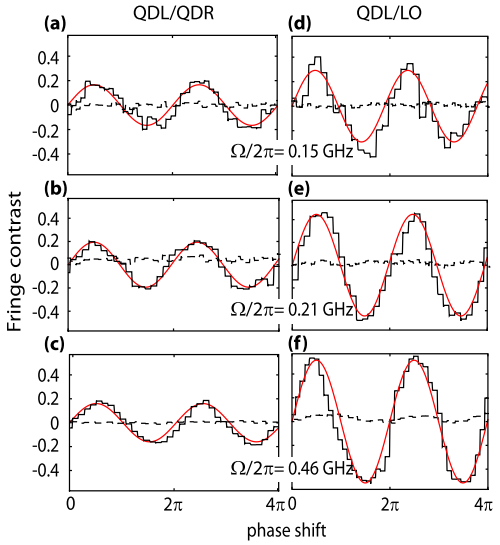

FIG. 3 (color online). (a)–(c) One-photon interference between light scattered by QDL and QDR for three different Rabi frequencies. (d)–(f) One-photon interference between light scattered by QDL and the local oscillator for the same Rabi frequencies. The dashed data lines were obtained with one of the input polarizations rotated by 90 deg.

Theoretical analysis.—We carried out a statistical analysis that accounts for the fluctuations of QD resonance frequencies due to spectral diffusion [14,23–26]. Spectral diffusion is often directly visible in the form of fluctuations of the scattered light intensity, as seen in Fig. 5(a). These fluctuations occur as a result of random Stark shifts, of magnitude δ_{Stark}, of the homogeneously broadened excitonic resonance. The homogeneous linewidth κ is set by radiative relaxation with decay constant $\tau = 1/\kappa$ [15,27]. Typically, $\tau \approx 0.9$ ns, so $\kappa/2\pi \approx 180$ MHz. The total scattered light intensity as a function of laser detuning (integrated over all detection frequencies) is then given by [2]

$$I_{\mathrm{tot}} = n_\infty = \frac{\Omega^2/4}{(\Delta\omega + \delta_{\mathrm{Stark}})^2 + \kappa^2/4 + \Omega^2/2}, \quad (1)$$

which is the population inversion at times long compared to the quantum evolution of the two-level system, but short compared to the spectral diffusion time scale. We thus assume a Stark shift that is static on the time scale of the quantum evolution of the two-level system, a justification for which can be found in Ref. [14]. The intensity of the coherent portion of the scattered light is given by [2]

$$I_{\mathrm{coh}} = |\alpha_\infty|^2 = \frac{\Omega^2}{4}\frac{(\Delta\omega + \delta_{\mathrm{Stark}})^2 + \kappa^2/4}{[(\Delta\omega + \delta_{\mathrm{Stark}})^2 + \kappa^2/4 + \Omega^2/2]^2}, \quad (2)$$

where α_∞ is the steady-state coherence of the two-level system.

Both linear and quadratic Stark shifts are found in QDs [28–30]. Thus, in general, $\delta_{\mathrm{Stark}}(V) \approx c_1 V + c_2 V^2$. If we assume that the electrical potential V at the location of the QD is fluctuating around zero (without loss of generality) following a normal distribution, $P_V(V) = e^{-V^2/2\sigma^2}/\sigma\sqrt{2\pi}$, then we can find the average value of the intensity as

$$\langle I_{\mathrm{tot}}(\Delta\omega)\rangle = \int g(V) P_V(V) dV, \quad (3)$$

where $g(V) = n_\infty[\delta_{\mathrm{Stark}}(V)]$. By comparison of Eq. (3) with the excitation spectra of Fig. 2(b), we obtain best fit parameters, c_1 and c_2, which are tabulated in Ref. [31]. There, a justification for our model is given and it is shown that, while the linear term in the Stark shift is dominating, the quadratic term gives rise to the slight asymmetry of the excitation spectra, visible in Fig. 2(b) for large Ω.

The distribution of the intensity of the scattered light is found as $P_I(I) = P_V[g^{-1}(I)]|\frac{d}{dI} g^{-1}(I)|$, where g^{-1} is the inverse of the function g. $P_I(I)$ is obtained experimentally as the histogram of the time trace in Fig. 5(a), shown in Fig. 5(b). The histogram closely follows the expected theoretical expression plotted as a solid red line in

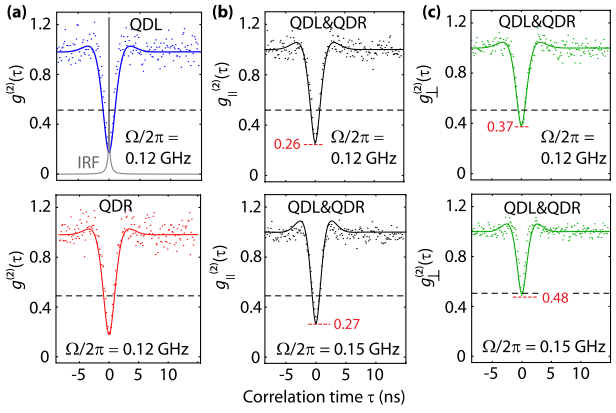

FIG. 4 (color online). (a) Second-order correlation function for the light scattered by QDL (top) and QDR (bottom). Measured average count rates at each detector were 3×10^4 s^{-1}. (b) Correlation function when light scattered from both QDL and QDR are entering the beam splitter. (c) Same but with the polarization of the two inputs perpendicular.

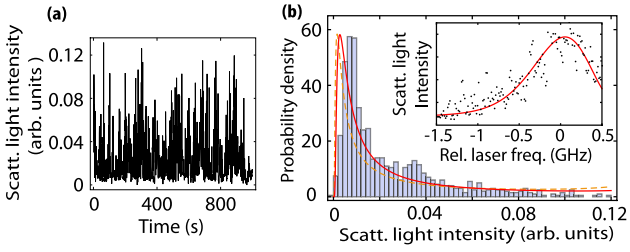

FIG. 5 (color online). (a) Temporal flickering of the scattered light for a QD in the same sample as QDL and QDR. (b) Histogram of the signal in (a), plotted together with theoretical probability distributions that assume a purely linear (solid red line) and a purely quadratic (dashed orange line) Stark shift. The inset shows the corresponding excitation spectrum and a theoretical fit.

TABLE I. Summary of one-photon interference visibilities.

$\Omega/2\pi$ (GHz)	Experimental		Theoretical		Theoretical (no spectral diffusion)	
	QD-LO	QD-QD	QD-LO	QD-QD	QD-LO	QD-QD
0.15	0.29	0.16	0.70	0.49	0.95	0.90
0.21	0.44	0.19	0.68	0.46	0.90	0.81
0.46	0.51	0.15	0.63	0.39	0.69	0.48

Fig. 5(b). With the distribution function, $P_I(I)$, we can calculate the theoretically expected fringe contrast for the data in Fig. 2. The one-photon fringe visibility $\mathcal{V}^{(1)}$ is given by the normalized first-order correlation function of the two fields at the beam splitter, as $\mathcal{V}^{(1)} = \langle U_1^* U_2\rangle/\sqrt{\langle I_1\rangle\langle I_2\rangle}$, where $U_k = A_k e^{-i\omega t}$ $(k = 1, 2)$ are the amplitudes of the electric field of the two waves entering the beam splitter. The corresponding average intensities are given by $I_k = \langle U_k^* U_k\rangle$. When one of the fields is the scattered light from a QD and the other is a local oscillator (LO) with the same average intensity, then

$$\mathcal{V}^{(1)}_{\mathrm{QD,LO}} = \frac{\langle\sqrt{I_{\mathrm{coh}}}\rangle}{\sqrt{\langle I_{\mathrm{tot}}\rangle}} = \frac{\int |\alpha_\infty[\delta_{\mathrm{Stark}}(V)]| P_V(V) dV}{\sqrt{\int n_\infty[\delta_{\mathrm{Stark}}(V)] P_V(V) dV}}. \quad (4)$$

Similarly, if the two fields correspond to the scattered light from QDL and QDR, respectively, with mutually uncorrelated intensity fluctuations, then $\mathcal{V}^{(1)}_{\mathrm{QDL,QDR}} = \langle\sqrt{I_{\mathrm{coh}}}\rangle^2/\langle I_{\mathrm{tot}}\rangle$. Using experimentally obtained values for $\Delta\omega$ and values for c_1, c_2, and σ that best match our excitation spectra of Fig. 2(b) and the statistical distribution of Fig. 5(b) [31], we obtain the values summarized in Table I.

Theoretical visibilities of the second-order interference experiment of Fig. 4 can be calculated in a similar manner, starting from an expression for the second-order correlation function written in terms of the autocorrelation functions of the constituent signals [7]. In particular, at $\tau = 0$, $g^{(2)}_\perp(0) = [I_L^2 g_L^{(2)}(0) + I_R^2 g_R^{(2)}(0) + 2I_L I_R]/(I_L + I_R)^2$ and $g^{(2)}_\parallel(0) = [I_L^2 g_L^{(2)}(0) + I_R^2 g_R^{(2)}(0)]/(I_L + I_R)^2$, where I_L (I_R) is the intensity of the light scattered from QDL (QDR) and $g_L^{(2)}(\tau)$ $[g_R^{(2)}(\tau)]$ the corresponding second-order autocorrelation function. With the known probability distribution function of Eq. (4), time averages, $\langle g^{(2)}_\perp(\tau)\rangle$ and $\langle g^{(2)}_\parallel(\tau)\rangle$, can be obtained as in Eq. (3). The theoretically calculated $\langle g^{(2)}_\perp(0)\rangle = 0.3$ $(\Omega/2\pi = 0.12$ GHz) is in close agreement with the observed value in the upper right-hand panel of Fig. 4.

Discussion.—Although our model does not precisely describe the experimental one-photon and two-photon visibility, it qualitatively captures its main limiting factors. In the absence of spectral diffusion, the one-photon interference visibility is expected to reach unity when $\Omega \ll \kappa$, i.e., when most of the light is scattered coherently, and vanish when $\Omega \gg \kappa$. Spectral diffusion affects this visibility by causing an increase in the fraction of coherently scattered light, as shown in Ref. [14], and by introducing a flickering of the scattered light intensity, which causes an "apparent" reduction in visibility due to variations in photon flux at the beam splitter. The two-photon interference visibility, on the other hand, is expected to be unity for any Ω, but is reduced in the presence of spectral diffusion due to variations in photon flux at the beam splitter. For large Ω, the two-photon visibility is further affected by the finite time resolution of our setup, which makes the value of $g^{(2)}(0)$ seem larger due to the reduction in width of the antibunching dip.

Note that our simplified model relies on a number of assumptions [31], ignoring anisotropic field fluctuations [32] and any contributions due to experimental factors such as interferometer misalignment or the fact that a small fraction of photons are always scattered incoherently due to interactions with phonons [33]. At 3.8 K, this fraction is about 5% [14].

Conclusion.—We have probed interference of photons scattered by two InAs QDs that are spatially well separated. Despite their atomlike behavior, QDs are highly sensitive to their solid-state environment, and small potential fluctuations can have a strong impact on their optical properties. Accordingly, we find fringe visibilities significantly reduced from unity. However, the source of this reduction is extrinsic in the sense that it is due to an averaging process over many random realizations of QD detunings due to spectral diffusion. With removal or circumvention of spectral diffusion, large visibilities may be expected, bringing about exciting opportunities for coherent control in solid-state systems. For example, with the neutral exciton transition replaced by a trion transition, remote entanglement of single spins may be achieved [5,6]. Like other approaches [34,35], the one presented here could forgo, possibly in a scalable manner, the need for tuning independent quantum systems into spectral resonance in order to obtain two-photon interference [7,10,11].

The authors acknowledge financial support from the National Science Foundation (NSF DMR-0906025 and CMMI-0928664) and the National Natural Science Foundation of China (Grant No. 90921015).

*mullera@usf.edu

[1] U. Eichmann, J. Bergquist, J. Bollinger, J. Gilligan, W. Itano, D. Wineland, and M. Raizen, Phys. Rev. Lett. **70**, 2359 (1993).
[2] B. R. Mollow, Phys. Rev. **188**, 1969 (1969).
[3] C. K. Hong, Z. Y. Ou, and L. Mandel, Phys. Rev. Lett. **59**, 2044 (1987).
[4] J. Beugnon, M. P. A. Jones, J. Dingjan, B. Darquié, G. Messin, A. Browaeys, and P. Grangier, Nature (London) **440**, 779 (2006).

[5] J. Hofmann, M. Krug, N. Ortegel, L. Gerard, M. Weber, W. Rosenfeld, and H. Weinfurter, Science **337**, 72 (2012).
[6] P. Maunz, D. L. Moehring, S. Olmschenk, K. C. Younge, D. N. Matsukevich, and C. Monroe, Nat. Phys. **3**, 538 (2007).
[7] R. Lettow, Y. L. A. Rezus, A. Renn, G. Zumofen, E. Ikonen, S. Götzinger, and V. Sandoghdar, Phys. Rev. Lett. **104**, 123605 (2010).
[8] C. Santori, D. Fattal, J. Vuckovic, G. S. Solomon, and Y. Yamamoto, Nature (London) **419**, 594 (2002).
[9] K. Sanaka, A. Pawlis, T. D. Ladd, K. Lischka, and Y. Yamamoto, Phys. Rev. Lett. **103**, 053601 (2009).
[10] E. B. Flagg, A. Muller, S. V. Polyakov, A. Ling, A. Migdall, and G. S. Solomon, Phys. Rev. Lett. **104**, 137401 (2010).
[11] R. B. Patel, A. J. Bennett, I. Farrer, C. A. Nicoll, D. A. Ritchie, and A. J. Shields, Nat. Photonics **4**, 632 (2010).
[12] H. Bernien, L. Childress, L. Robledo, M. Markham, D. Twitchen, and R. Hanson, Phys. Rev. Lett. **108**, 043604 (2012).
[13] H.-J. Briegel, W. Dür, J. I. Cirac, and P. Zoller, Phys. Rev. Lett. **81**, 5932 (1998).
[14] K. Konthasinghe *et al.*, Phys. Rev. B **85**, 235315 (2012).
[15] P. Borri, W. Langbein, S. Schneider, U. Woggon, R. L. Sellin, D. Ouyang, and D. Bimberg, Phys. Rev. Lett. **87**, 157401 (2001).
[16] A. Muller, E. B. Flagg, P. Bianucci, X. Y. Wang, D. G. Deppe, W. Ma, J. Zhang, G. J. Salamo, M. Xiao, and C. K. Shih, Phys. Rev. Lett. **99**, 187402 (2007).
[17] E. B. Flagg, A. Muller, J. W. Robertson, S. Founta, D. G. Deppe, M. Xiao, W. Ma, G. J. Salamo, and C. K. Shih, Nat. Phys. **5**, 203 (2009).
[18] G. Wrigge, I. Gerhardt, J. Hwang, G. Zumofen, and V. Sandoghdar, Nat. Phys. **4**, 60 (2007).
[19] A. N. Vamivakas, Y. Zhao, C.-Y. Lu, and M. Atatüre, Nat. Phys. **5**, 198 (2009).
[20] S. Ates, S. Ulrich, S. Reitzenstein, A. Löffler, A. Forchel, and P. Michler, Phys. Rev. Lett. **103**, 167402 (2009).
[21] H. S. Nguyen, G. Sallen, C. Voisin, Ph. Roussignol, C. Diederichs, and G. Cassabois, Appl. Phys. Lett. **99**, 261904 (2011).
[22] C. Matthiesen, A. N. Vamivakas, and M. Atatüre, Phys. Rev. Lett. **108**, 093602 (2012).
[23] A. Högele, S. Seidl, M. Kroner, K. Karrai, R. Warburton, B. D. Gerardot, and P. M. Petroff, Phys. Rev. Lett. **93**, 217401 (2004).
[24] C. Santori, D. Fattal, J. Vučković, G. S. Solomon, E. Waks, and Y. Yamamoto, Phys. Rev. B **69**, 205324 (2004).
[25] C. Latta *et al.*, Nat. Phys. **5**, 758 (2009).
[26] H. S. Nguyen, G. Sallen, C. Voisin, Ph. Roussignol, C. Diederichs, and G. Cassabois, Phys. Rev. Lett. **108**, 057401 (2012).
[27] W. Langbein, P. Borri, U. Woggon, V. Stavarache, D. Reuter, and A. Wieck, Phys. Rev. B **70**, 033301 (2004).
[28] B. Alén, F. Bickel, K. Karrai, R. J. Warburton, and P. M. Petroff, Appl. Phys. Lett. **83**, 2235 (2003).
[29] B. D. Gerardot *et al.*, Appl. Phys. Lett. **90**, 041101 (2007).
[30] M. M. Vogel, S. M. Ulrich, R. Hafenbrak, P. Michler, L. Wang, A. Rastelli, and O. G. Schmidt, Appl. Phys. Lett. **91**, 051904 (2007).
[31] See Supplemental Material at http://link.aps.org/supplemental/10.1103/PhysRevLett.109.267402 for details on theoretical modeling.
[32] B. Patton, W. Langbein, and U. Woggon, Phys. Rev. B **68**, 125316 (2003).
[33] L. Besombes, K. Kheng, L. Marsal, and H. Mariette, Phys. Rev. B **63**, 155307 (2001).
[34] S. V. Polyakov, A. Muller, E. B. Flagg, A. Ling, N. Borjemscaia, E. Van Keuren, A. Migdall, and G. Solomon, Phys. Rev. Lett. **107**, 157402 (2011).
[35] S. Ates, I. Agha, A. Gulinatti, I. Rech, M. Rakher, A. Badolato, and K. Srinivasan, Phys. Rev. Lett. **109**, 147405 (2012).